SAND2013-3439C

Numerical Simulation of Decomposition and Combustion of an Epoxy-Carbon-Fiber Composite*

A. B. Dodd, B. Shelden*, and K. L. Erickson**
Sandia National Laboratories, Livermore, CA 94551
*Sandia National Laboratories, Albuquerque, NM, USA 87185
**Consultant, Albuquerque, NM, USA, 87199

ABSTRACT

In fire environments, composite materials behave differently from conventional fuel sources and have the potential to smolder and burn for extended time periods. Thermal decomposition and oxidation of carbon-fiber composite materials were investigated using multiple techniques. Resulting data were used to develop thermal property and chemical reaction rate expressions that are suitable for use in numerical simulations of the fire behavior of such materials in large structures in a variety of hazard scenarios.

INTRODUCTION

In fire environments, composite materials behave differently from conventional fuel sources and have the potential to smolder and burn for extended time periods. As the amount of composite materials on modern aircraft continues to increase, understanding the response of composites in fire environments becomes increasingly important. Thermal decomposition and oxidation of carbon-fiber composite materials were investigated to obtain data for developing thermal property and chemical reaction rate expressions that are suitable for use in numerical simulations of the fire behavior of such materials in large structures in a variety of hazard scenarios. This paper summarizes results from experiments with epoxy-carbon-fiber composites (Cytec Industries 977-3 unidirectional and 977-3 woven). Most results discussed below were obtained using the unidirectional material. Experimental techniques, the resulting data, and evaluation of reaction rate expressions and thermal properties are discussed first. Incorporation of those results into numerical models for simulating composite panel experiments is then illustrated.

EXPERIMENT

Most experimental data were obtained by thermal gravimetric analysis (TGA) using open platinum pans. Simultaneous TGA-FTIR was used to examine evolved gases. Samples were thin square sheets about 2 mm on a side. The TGA purge gas was UHP N_2, high purity air, 95%N_2-5%O_2, or 98%N_2-2%O_2 flowing at 35 ml/min. Multiple heating programs were used and included: (1) constant heating rate of 1/30 K/s to 25/3 K/s (2 to 500 K/min) and (2) constant heating rate followed by isothermal heating at temperatures from 723 K to 923 K. Simultaneous TGA-DSC (SDT) with samples in open ceramic pans and air or 95%N_2-5%O_2 purge was used to evaluate enthalpy changes resulting from oxidation at temperatures from 473 K to 1273 K. Differential scanning calorimetry (DSC) with N_2 purge and samples in open gold pans was used to obtain data for evaluating specific heat and heat of gasification at temperatures from ambient to 973 K.

* Sandia is a multi-program laboratory operated by Sandia Corporation, a Lockheed Martin Company, for the United States Department of Energy's National Nuclear Security Administration under Contract DE-AC04-94AL85000.

THERMAL GRAVIMETRIC ANALYSIS AND DEVELOPMENT OF RATE EXPRESSIONS

Results from replicate constant heating rate experiments in N_2 are shown in Fig. 1. Mass loss is due to thermal decomposition of the epoxy binder and was 22% to 24% of the initial sample mass. Similar experiments with only the epoxy binder showed that about 76% to 82% of the epoxy ultimately evolved to the gas phase. The other 18% to 24% formed char. In general, as the heating rate increased, the amount of char that formed decreased slightly. Constant heating rate experiments also were done with the epoxy binder using air, 95%N_2-5%O_2, and 98%N_2-2%O_2 purge gas. Results from those experiments showed that the amount of char that formed: (1) increased substantially as O_2 concentration increased, (2) decreased as heating rate increased, and (3) was significant at low O_2 concentrations.

Results from replicate constant heating rate experiments in air are illustrated in Fig. 2. Depending on heating rate: (1) the mass loss that occurred between temperatures of 600 K and 800 K was 10% to 14 % of the original sample mass and was due to decomposition of the epoxy binder; (2) additional mass loss then occurred slowly between temperatures of 700 K and 850 K; (3) between temperatures of 850 K and 1000 K, the rate of mass loss increased and the mass loss curves shifted substantially with heating rate, and (4) at temperatures of about 875 K and higher (at mass loss between 30% and 40%) the rate of mass loss greatly increased. Based on the above results, it appeared that the following mechanisms were responsible for depletion of the composite samples: (1) thermal decomposition of the epoxy binder with concurrent formation of char, which decomposed (or oxidized) slowly until temperatures exceeded 850 K; (2) subsequent oxidation of the char formed from the epoxy, and (3) oxidation of the carbon fibers, which appeared to occur by two mechanisms having significantly different temperature dependence.

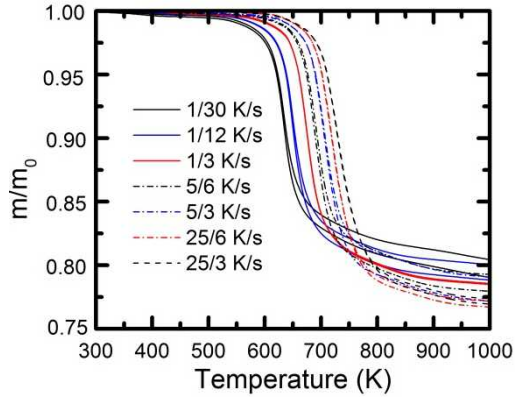

Figure1. TGA: constant heating rate, N_2 purge.

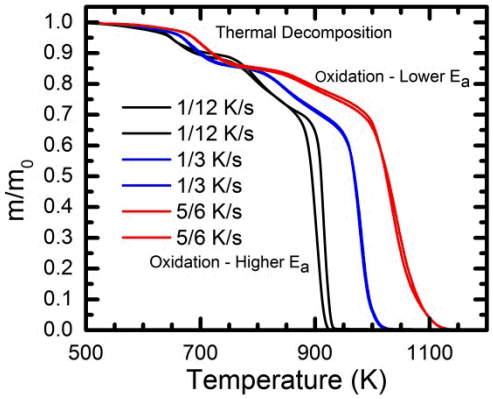

Figure 2. TGA: constant heating rate, air purge.

In the TGA curves in Fig. 2, the substantial shift with heating rate was attributed to an oxidation reaction that was much less temperature dependent, having lower activation energy E_a, than the rapid reaction, having higher activation energy, that consumed the major portion of each sample, particularly the carbon fibers. Furthermore, spectra obtained from simultaneous TGA-FTIR experiments indicated that the lower-activation-energy reaction produced a much higher ratio of CO/CO_2 than the higher-activation-energy reaction produced.

Initial rate expressions were developed assuming first order reactions with respect to the mass of binder, mass of carbon fibers, and O_2 mass fraction relative to that in air. The composite material was considered to be 40% by mass epoxy binder and 60% carbon fibers. Rate constants for the thermal decomposition of the epoxy binder in N_2 were determined using the data in Fig. 1. Rate constants for the thermal decomposition of the epoxy binder in O_2 were determined using the data in Fig. 2. Rate constants for the higher-activation-energy carbon fiber oxidation reaction were determined using the data in Fig. 2. Rate constants for the lower-activation-energy carbon fiber oxidation reaction were determined using the data in Fig. 2 and using data from a series of two-step experiments: (1) constant heating at 1/3 K/s to 873 K, then isothermal until mass m/m_0 decreased to 0.60, followed by cooling to

ambient, and (2) heating at 1/3 K/s to temperatures of 723 K to 923 K, then isothermal until samples were consumed. The two-step experiments were done using air, 95%N_2-5%O_2, and 98%N_2-2%O_2 purge gas. Results from the second isothermal step are shown in Fig. 3 for experiments with air. Similar two-step experiments with the epoxy binder examined oxidation of the epoxy char.

An Arrhenius plot of the rate constants obtained from the data in Fig. 3 is shown in Fig. 4. The resulting value of E_a/R was 12,100 K, as compared with 38,000 K that was determined for the higher-activation-energy oxidation reaction. Similar analysis of data from the two-step experiments using 95%N_2-5%O_2 and 98%N_2-2%O_2 purge gas indicated that oxidation was approximately first order in the O_2 mass fraction relative to air. Figure 5 compares the resulting rate expression (E_a/R = 27,200 K) for decomposition of the epoxy with the data in Fig. 1, which were normalized to the final mass of each sample. Figure 6 provides a comparison of experimental data with the corresponding mass loss curve predicted by combining rate expressions for decomposition and oxidation reactions.

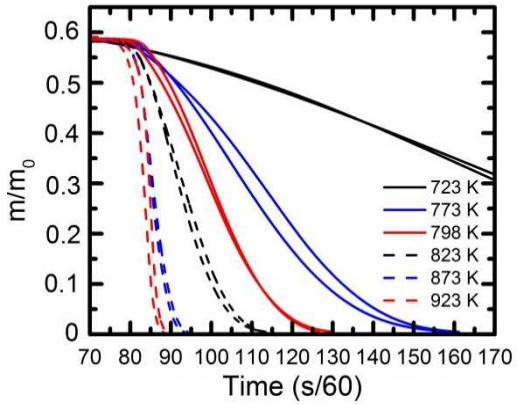

Figure 3. Step 2 "isothermal" experiments.

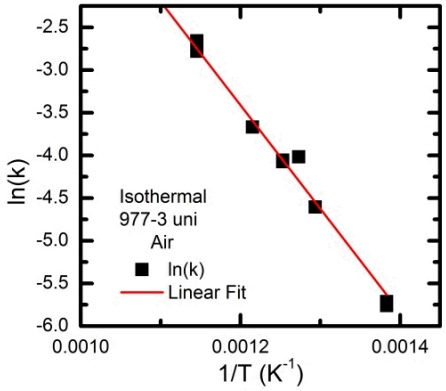

Figure 4. Arrhenius plot.

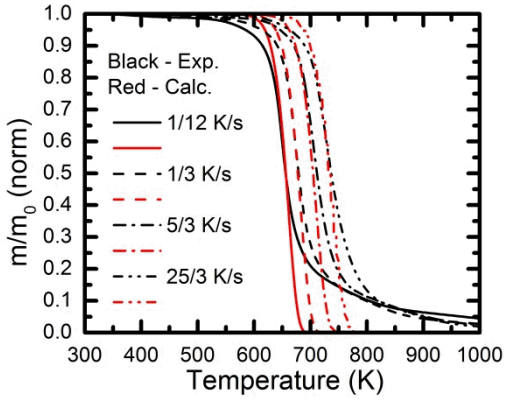

Figure 5. Epoxy decomposition: exp. vs. calculation.

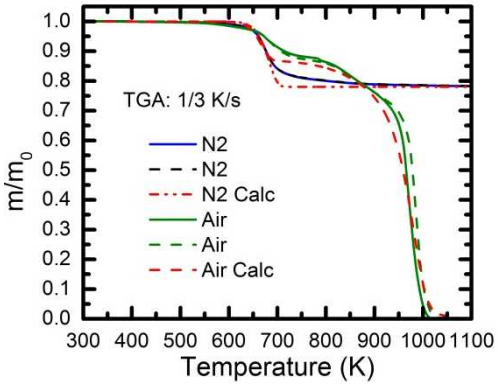

Figure 6. Composite: exp. vs. calculation.

DIFFERENTIAL SCANNING CALORIMETRY AND THERMAL PROPERTIES

Simultaneous TGA-DSC (SDT)

Results from replicate simultaneous TGA-DSC (SDT) experiments are shown in Fig. 7. The experiments were done using air as the purge gas. Samples were heated at 1/3 K/s (20 K/min). Figure 7a shows the measured heat flow Q (kW/kg) versus temperature. Figure 7b shows the corresponding rate of the relative mass (m/m_0) loss versus temperature. Figures 8a and 8b show the analogous data from Sample 2 as a function of time. Figure 9 compares the mass loss results from the SDT experiments with the corresponding results from the TGA experiments shown in Fig. 2. The agreement between replicate experiments involving two very different instruments is very good. In Fig. 7a, net exothermic heat flow is not significant until temperatures above 775 K and corresponds to the two oxidation reactions mentioned above. In Fig. 8a, the smaller peak labeled "2" corresponds to

the lower-activation-energy reaction which produces mostly CO. The much larger peak labeled "4" corresponds to the higher-activation-energy reaction that produces mostly CO_2. The heat of reaction ΔH_i for both reactions was estimated using two methods: (1) the ratio of maximum heat flow Q_{max} at each peak to the corresponding rate of mass loss $d(m/m_0)/dt$, and (2) the ratio of the integral of heat flow Q over a selected time interval $\int_{t_i}^{t_{i+1}} Q dt$ to the corresponding change in mass $[(m/m_0)_{i+1} - (m/m_0)_i]$. For the smaller peak, the time interval corresponded to the time between labels "1" and "2". For the larger peak, the time interval corresponded to the interval labeled "3." The cumulative integral, with respect to time, of net exothermic heat flow is shown in Fig. 10.

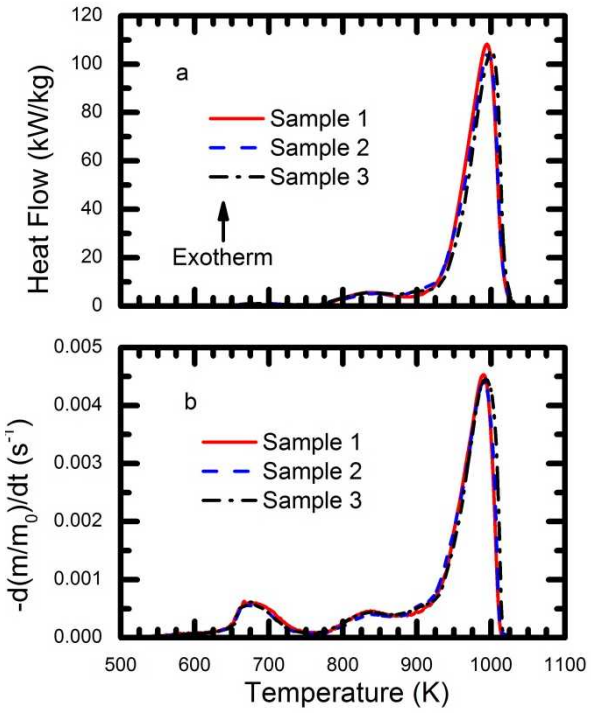

Figure 7. Simultaneous TGA-DSC results

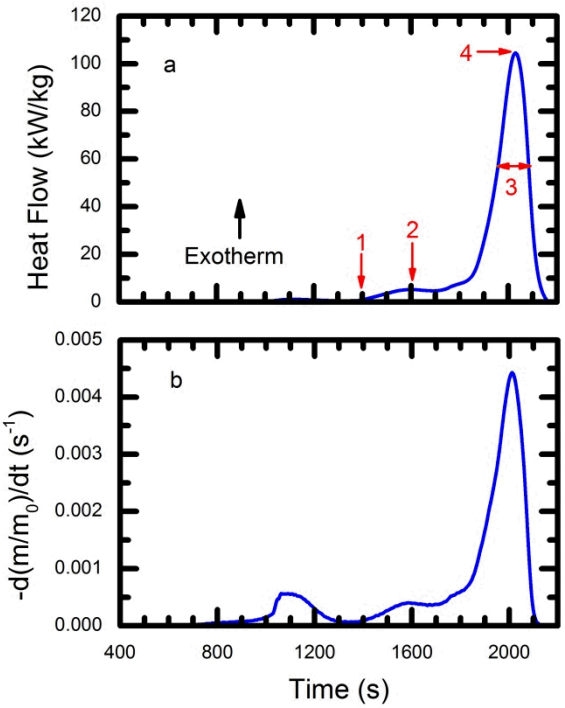

Figure 8. Results from sample 2 (Fig. 7).

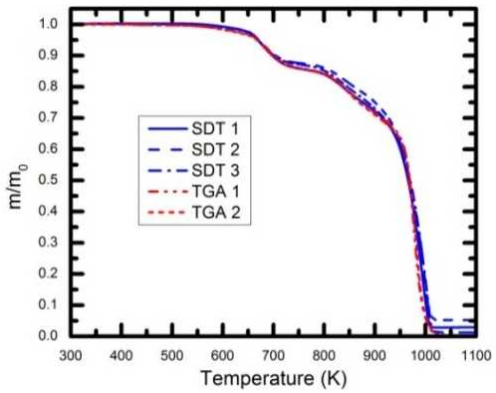

Figure 9. SDT and TGA results compared.

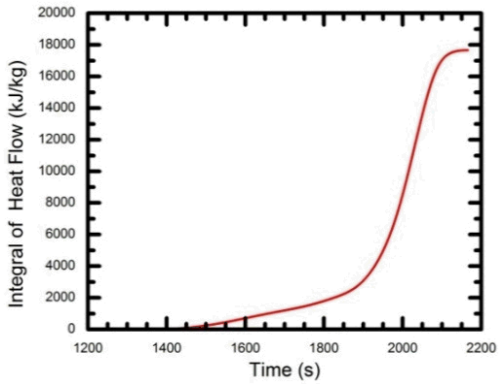

Figure 10. Cumulative integral of heat flow.

Values calculated for ΔH_1 and ΔH_2 are summarized in Table 1. For comparison, the heat of formation of CO at temperatures between 700 K and 1100 K varies from 9.20 x 10^3 to 9.37 x 10^3 kJ/kg of carbon, and the heat of formation of CO_2 varies from 32.80 x 10^3 to 32.87 x 10^3 kJ/Kg of carbon[1].

Table 1. Values calculated for ΔH_1 and ΔH_2 using Method1 and Method 2.

	ΔH_1 (kJ/kg)		ΔH_2 (kJ/kg)	
Sample	Method 1	Method 2	Method 1	Method 2
1	12,230	12,630	24,910	24,930
2	13,270	12,770	25,000	24,730
3	12,710	12,760	24,860	24,190
Average	12,740	12,720	24,920	24,620
Average	12,730		24,770	

Differential Scanning Calorimetry (DSC)

Replicate DSC experiments were done with both unidirectional and woven samples. Results from experiments with unidirectional samples varied substantially. Results from the larger woven samples, were more consistent and are shown in Fig. 11. Each of the two samples was subjected to three identical heating cycles: heating at 1/3 K/s and then cooling to ambient temperature before reheating. Decomposition of the epoxy binder occurred during Run 1. At temperatures above 500 K, the net heat flow remains endothermic due to absorption of sensible and latent heat. However, the three distinct local minima indicate exothermic effects. The local minimum at about 550 K may result from some higher temperature curing of the epoxy. Mass loss due to thermal decomposition of the epoxy binder begins at temperatures of about 600 K and would result in some "apparent exothermic'' behavior. But the effect would be less significant than is indicated by the results observed above 600 K.

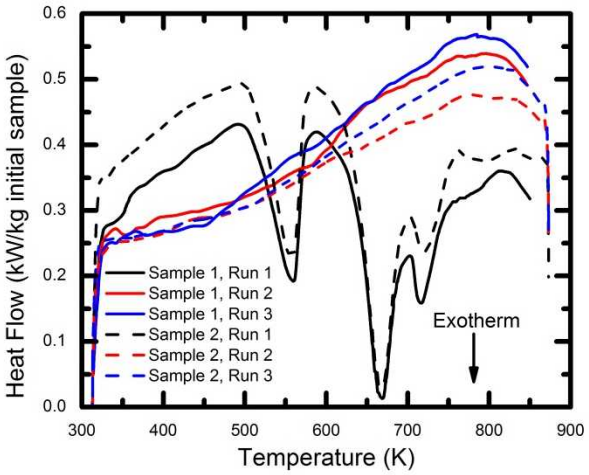

Figure11. DSC Results (endotherm up).

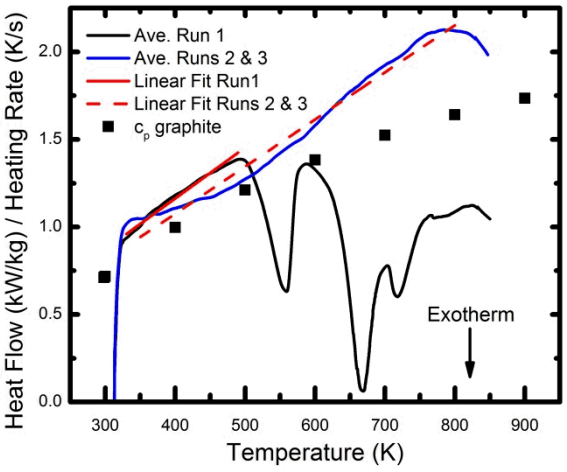

Figure 12. Heat capacity (endotherm up).

Figure 12 shows the average of the Run 1 results and the average of the Run 2 and Run 3 results. In both cases, the average values have been divided by the heating rate of 1/3 K/s. Also, the Run 2 and Run 3 data have been divided by 0.74, the average value of m/m_0 at the end of Run 3. In the region between 330 K and 490 K, the Run 1 results represent the heat capacity of the initial composite material prior to decomposition. A linear fit ($c_p = aT$, where $a = 0.00291\ \mathrm{kJ/kgK}$) to that data is shown in Fig. 12. Ideally, the results from Runs 2 and Runs 3 represent heat capacity of the residue (carbon fibers and epoxy char) remaining after decomposition of the binder. However, in Figure 11, it appears that during reheating, some exothermic effects occur as temperatures increase above 600 K. At the higher temperatures, the heat flow during Run 2 is always slightly less than the heat flow during Run 3. The average of the Run 2 and Run 3 results, between 330 K and 890 K, is shown in Figure 12. A linear fit ($c_p = aT$, where $a = 0.00269\ \mathrm{kJ/kgK}$) to that data is shown in Figure 12. For comparison, data for the heat capacity of graphite[2] are included in Figure 12.

NUMERICAL MODELING

As illustrated in the previous sections, a substantial amount of effort has been performed to develop a decomposition model incorporating both thermal and oxidative processes. A preliminary effort to implement this model to simulate scenarios of interest such as decomposition and burning of a composite material subjected to fire-like heat fluxes is demonstrated. The numerical model consists of coupling a heat transfer, thermal and oxidative pyrolysis model that simulates the composite material behavior to a computational fluid dynamics (CFD) representation of the gas-phase. The decomposition model has been implemented the generalized pyrolysis model, Gpyro[3], which is coupled to FDS[4] that simulates the CFD response. The details of the governing equations and numerical solution methodology can be found in Lautenberger and Pello[5]. The computational domain is a simplified representation of an experiment presented in Hubbard *et al.*[6]. The fluid domain is 0.4 m wide by 0.14 m tall. The radiant heat source is represented by a heated surface 0.19 m wide on the boundary of the fluid domain. The composite is 0.102 m wide and 0.0032 m thick with an insulated boundary condition at the bottom of the domain. Figure 13 shows the temperature field during epoxy binder decomposition, prior to gas phase ignition. Figure 14 shows the temperature field after ignition has occurred in the gas-phase region. The model provides a favorable qualitative comparison to experimental data representing the physics that describe decomposition, heat transfer, and flaming of a composite material subjected to an incident heat flux. Additional effort performing detailed quantitative comparisons will be the focus of future work.

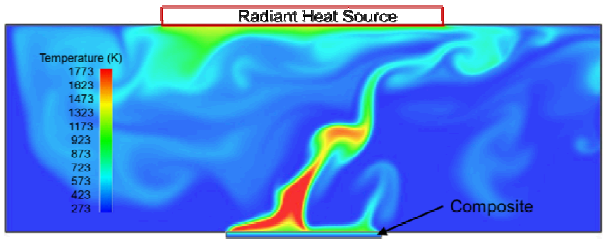

Figure 13. Temperature field during epoxy binder decomposition.

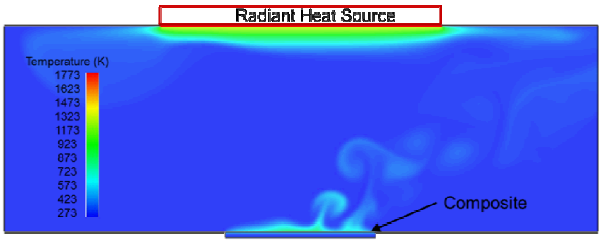

Figure 14. Temperature field after gas-phase ignition has occurred.

ACKNOWLEDGEMENTS

The authors gratefully acknowledge the assistance of Alex Brown of Sandia National Laboratories.

REFERENCES

1. *Handbook of Chemistry and Physics 73rd Edition*, CRC Press, David R. Lide, Editor in Chief, Boca Raton (1992), p. 5-54.

2. *Ibid*, p. 5-53.

3. http://reaxengineering.com/trac/gpyro

4. McGrattan, K., McDermott, R., Hostikka, S., Floyd, J. Fire Dynamics Simulator (Version 5) User's Guide, NIST Special Publication 1019-5, 2010.

5. Lautenberger, C. and Fernandez-Pello, A.C., "Modeling Ignition of Combustible Fuel Beds by Embers and Heated Particles," *Forest Fires 2008*, 2008.

6. Hubbard, J.A., Brown, A.L., Dodd, A.B., Gomez-Vasquez, S., and Ramirez, C.J. "Aircraft carbon fiber composite characterization in adverse thermal environments: radiant heat and piloted ignition flame spread," Sandia Report SAND2011-2833, 2011.